Research Article ISSN 2771-9057

Recent Advances in Clinical Trials

Spinal Impedance Matching: A First-Principles Model for Proximal Adjacent Vertebra Augmentation

Chi-Ming Chiang, MD, PhD[1,2*]

[1]*Center for General Education, Chung Yuan Christian University, Taoyuan, Taiwan, China.*

[2]*Department of Orthopedics, Yi-Her Hospital, Choninn Medical Group, New Taipei City, Taiwan, China.*

***Correspondence:**

Chi-Ming Chiang, MD, PhD, Center for General Education, Chung Yuan Christian University, Taoyuan, Taiwan, China.

Received: 29 Nov 2025; **Accepted:** 22 Dec 2025; **Published:** 31 Dec 2025

Citation: Chi-Ming Chiang. Spinal Impedance Matching: A First-Principles Model for Proximal Adjacent Vertebra Augmentation. Recent Adv Clin Trials. 2025; 5(6): 1-5.

ABSTRACT

Background: *Junctional complications after posterior lumbar instrumentation cluster at the construct's cranial border, where a rigid metal–bone subsystem must couple to a compliant osteoligamentous column. This transition behaves as a mechanical "stress singularity" (a stiffness cliff) that concentrates bending moments and micro-motion at the uppermost instrumented vertebra (UIV), yet the clinical phenotype remains variable and seemingly stochastic.*

Objective: *To develop a deterministic, mechanics-first rationale for prophylactic augmentation of the proximal adjacent vertebra (UIV+1), treating the junction as an impedance-matching problem. The goal is not to further stiffen the hardware, but to increase the stiffness of the adjacent vertebral body and thereby smooth the stiffness gradient at the interface.*

Methods: *Two compact models were derived. (1) A parallel rotational-spring (moment-sharing) model partitions an applied sagittal moment between the UIV screw–rod complex (rotational stiffness K_s) and the cranial functional unit (K_a), yielding M_s/M_appl = K_s/(K_s+K_a) (Eq. 1). Augmenting UIV+1 multiplies K_a by α>1 and reduces the screw-borne moment by ρ = (K_s+K_a)/(K_s+αK_a) (Eq. 2). (2) A beam-on-elastic-foundation (BOEF) model describes cranial load transfer with characteristic length ℓ = (EI/k)^{1/4} (Eq. 3); increasing local foundation stiffness k→αk shortens the load-transfer zone, ℓ→ℓ·α^{−1/4}. The framework was applied to an early radiographic series using low-temperature, high-viscosity polymethylmethacrylate (PMMA) injected into UIV+1.*

Results: *The derivations predict monotonic offloading of the UIV screw as α increases and a shorter cranial stress-transfer region after augmentation. Early radiographs demonstrate contained cement filling, preserved proximal disc/endplate geometry, and absence of radiographic screw toggling in illustrated cases.*

Conclusion: *Proximal junctional failure can be reframed as a predictable consequence of impedance mismatch at a stiffness discontinuity. UIV+1 cement augmentation provides a deterministic, physics-guided design strategy to smooth this transition, redistribute moments away from the UIV screw, and localize load transfer, potentially reducing junctional failure without extending the construct.*

Keywords

Stress singularity, Impedance matching, First principles, UIV+1, Proximal adjacent vertebra, Moment sharing, Beam on elastic foundation, Spinal mechanics, PMMA.

Introduction

Proximal junctional complications after posterior lumbar fixation—ranging from symptomatic proximal screw loosening to adjacent vertebral collapse and progressive junctional kyphosis—are often attributed to frailty, osteoporosis, or "tissue quality". Those factors matter, but they act on a boundary condition that is imposed by instrumentation: the cranial end of a rigid construct must couple to the mobile spine. Across spine literature, prophylactic vertebroplasty at the UIV and/or UIV+1 has been

explored as one mechanical means of reducing junctional failure, with mixed but encouraging signals in selected series [1-3], and broader prevention strategies have been summarized in systematic review form [4].

Two common surgical responses to impending junctional problems also expose a central mechanical dilemma. Extending instrumentation cranially can reduce local loads but increases operative morbidity, implant burden, and adjacent-level sacrifice. Cement-augmenting proximal screws can improve fixation strength, yet by increasing stiffness on the rigid side of the border it may steepen the stiffness gradient and shift injury to the adjacent uninstrumented segment; cement-augmented pedicle screws also carry distinct complication profiles [5].

In this technical report with analytic modeling, we propose a different target: the vertebral body immediately cranial to the UIV (UIV+1), referred to here as the proximal adjacent vertebra (PAV). Instead of hardening the construct, we modestly stiffen the adjacent vertebral body using low-temperature, high-viscosity polymethylmethacrylate (PMMA). The central hypothesis is that this acts as impedance matching—smoothing the stiffness cliff at the junction—thereby reducing the moment demand on the UIV screw–rod complex and shortening the cranial region over which bending is transferred. To avoid purely empirical argumentation, we derive two simplified but falsifiable models that quantify these effects and then map their predictions to radiographic surrogates.

Conceptual framework: smoothing a stiffness cliff by impedance matching

At the construct's cranial edge, sagittal moments generated by posture and gait propagate along the rod and must be equilibrated by the adjacent spinal column. If the cranial functional unit is compliant—because of low bone density, insufficiency of trabecular architecture, or laxity of the disc–ligament complex—then a large fraction of the applied moment is resisted by the UIV screw–rod complex, promoting cyclic micro-rotation ("toggling"), progressive endplate encroachment, and eventual loosening or adjacent failure.

This border can be conceptualized as a stress singularity: an interface where a sharp change in stiffness produces a sharp change in internal force distribution, with peak stresses localized near the junction. Although "singularity" is not meant here as a literal mathematical divergence, it usefully emphasizes that the location of maximal risk is structurally determined, while the biological expression of failure is patient-specific. From an interface-mechanics standpoint, the junction resembles an impedance mismatch: a high-impedance element (instrumented segment) couples to a low-impedance element (cranial spine), and the mismatch amplifies local response. The practical implication is that interventions should aim to smooth the stiffness gradient rather than to further stiffen the rigid subsystem.

UIV+1 vertebral augmentation offers a direct way to increase the stiffness of the cranial element. If a modest increase in adjacent vertebral stiffness can shift a measurable fraction of moment from the UIV screw to the cranial unit, then the UIV screw experiences fewer damaging micro-motions per loading cycle. In addition, if the augmentation increases local foundation stiffness for the cranial column, the length scale over which the rod-generated deformation is transmitted cranially should shrink, potentially reducing disc and ligament strain.

Methods

This work is presented in a dual-track format: a mechanics-first derivation intended to yield transparent predictions, and a clinician-facing description of technique and measurement surrogates.

Moment-sharing model (parallel rotational springs). The proximal border is modeled as two rotational springs acting in parallel under small sagittal rotations. The UIV screw–rod complex has rotational stiffness K_s, and the cranial functional unit (UIV–UIV+1 motion segment, dominated by the adjacent vertebral body, disc, and ligaments) has rotational stiffness K_a. Under an applied moment M_appl producing a rotation θ, the resisting moments are M_s = K_s·θ and M_a = K_a·θ, so M_appl = (K_s+K_a)·θ. Therefore, the fraction of the applied moment borne by the screw–rod complex is:

$$M_s / M_{appl} = K_s / (K_s + K_a) \quad \text{(Eq. 1)}$$

Augmenting UIV+1 is modeled as multiplying the cranial stiffness by α>1, so K_a→αK_a. The reduction factor for screw-borne moment is:

$$\rho := M_s(\alpha) / M_s(1) = (K_s + K_a) / (K_s + \alpha K_a) \quad \text{(Eq. 2)}$$

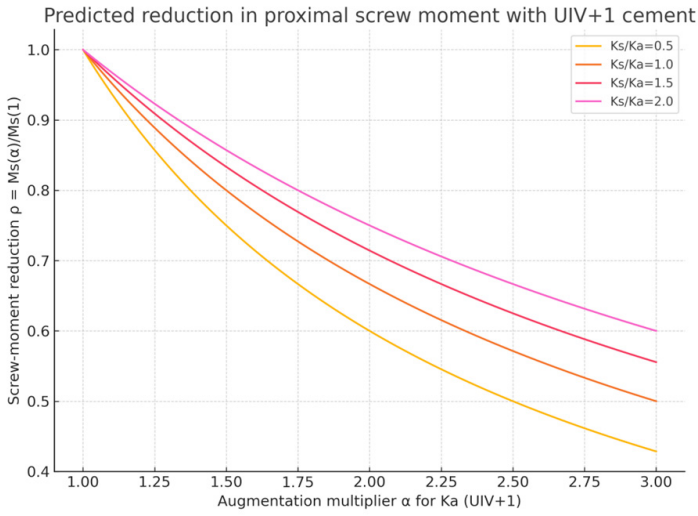

Figure 1: Predicted reduction in proximal screw moment. The reduction factor ρ = Ms(α)/Ms(1) decreases with the augmentation multiplier α for Ka. Curves shown for different Ks/Ka ratios (Eq. 2).

Beam-on-elastic-foundation (BOEF) model. The cranial spine is idealized as a beam of flexural rigidity EI resting on an elastic foundation of stiffness k representing the distributed support of

vertebral bodies and surrounding tissues. In small-deflection form, EI·y"" + k·y = q(x). The characteristic load-transfer length is:

$$\ell = (EI / k)^{(1/4)} \quad \text{(Eq. 3)}$$

After augmentation, local foundation stiffness is increased (k→αk), so ℓ→ℓ·α^(−1/4). This predicts that local stiffening will confine deformation and reduce cranial propagation of junctional strain.

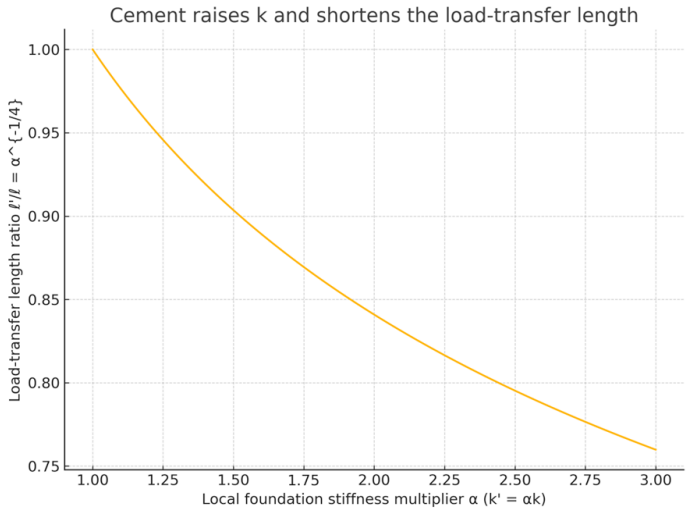

Figure 2: Load-transfer length shortens with cement. In a BOEF model, ℓ′/ℓ = α^(−1/4) where α is the multiplier of local f^ (nidation stiffness k at UIV+1 (Eq. 3).

Clinical technique (early radiographic experience). In illustrated cases, prophylactic augmentation targets the vertebral body immediately cranial to the UIV (UIV+1). Low-temperature, high-viscosity PMMA is utilized to facilitate controlled injection and cement containment, features associated with reduced leakage in vertebroplasty literature [6,7], while low-exotherm/thermal-safety considerations support the choice of low-temperature formulations [8]. Cement is injected to centrally reinforce trabecular bone, aiming to increase K_a and k without violating the endplates. AP and lateral radiographs are used to document cement distribution and junctional alignment.

Radiographic surrogates and planned endpoints. Standing lateral radiographs permit measurement of (i) the UIV–UIV+1 segmental wedge angle (Δφ), (ii) the minimal distance from the screw head to the superior endplate (d_head–EP), and (iii) proximal halo formation (binary or graded). AP radiographs assess vertebral body height symmetry and cement containment. Early clinical endpoints proposed for subsequent study include 24/48/72-hour pain (VAS), time to unaided corridor ambulation, and length of stay, with analyses adjusted for age, T-score, construct length, and alignment parameters.

Clinical Application

Imaging Examples representative AP and lateral radiographs from patients treated with adjacent (UIV+1) cement augmentation. The model predicts smaller Δφ, larger d_head–EP, less halo formation, and earlier mobilization compared to non-augmented controls. Here we put emphasis on the analytic framework and its clinical translation.

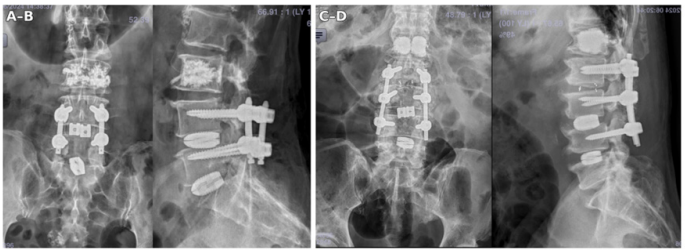

Figure 3: Two representative cases. Left panel ("A–B"): Case 1 (AP/Lateral). Right panel ("C–D"): Case 2 (AP/Lateral). Both demonstrate UIV+1 cement augmentation with maintained screw seating and minimal proximal interspace wedging.

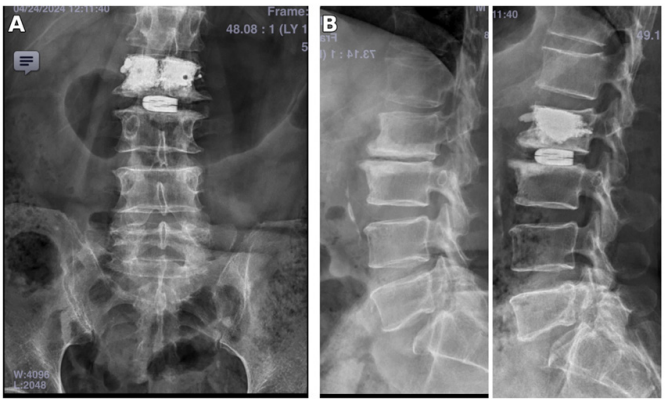

Figure 4: Case 3 Before/after lateral and confirmatory AP following UIV+1 augmentation. Lateral panels (B left: pre-augmentation; right: post-augmentation) show increased vertebral body opacity and preserved alignment; A: AP confirms midline distribution.

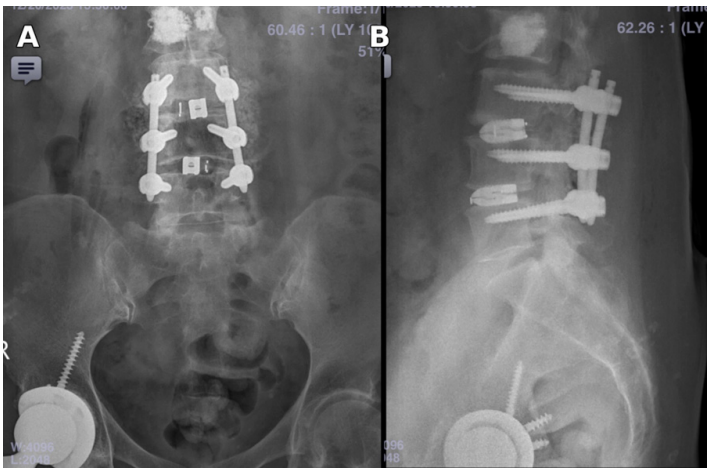

Figure 5: Case 4 (A) AP and (B) lateral views again demonstrate augmenting the first cranial adjacent vertebra instead of extending the construct; the proximal screw remains seated without superior encroachment.

Results

The first-principles derivations yield two monotonic, testable predictions.

First, Eq. (2) predicts that increasing adjacent cranial stiffness reduces screw-borne moment. If $K_s \approx K_a$, then $\alpha=2$ produces $\rho=2/3$, corresponding to an approximate 33% reduction in M_s; $\alpha=3$ produces $\rho=1/2$, a 50% reduction. In practical terms, even moderate increases in cranial stiffness should reduce cyclic micro-rotation at the screw–bone interface, which is the mechanical substrate of toggling and progressive loosening.

Second, the BOEF model predicts localization of load transfer: increasing k decreases ℓ as $\alpha^{-1/4}$. Because the exponent is small, substantial stiffening yields modest length-scale changes (e.g., doubling k shortens ℓ by ≈16%), yet those changes may matter in a region where disc, ligament, and endplate tissues are close to failure thresholds.

In the illustrative radiographic series, cement distribution remains confined to the UIV+1 vertebral body with no obvious endplate violation in the presented examples. Lateral films show preserved proximal disc/endplate geometry and absence of radiographic halo around the UIV screws in illustrated follow-up views. These observations are consistent with the predicted offloading and localization effects, though they remain qualitative surrogates pending a controlled cohort analysis.

Discussion

The proximal junction is most usefully treated as an interface problem: junctional complications arise where a stiff construct meets a compliant spine. By explicitly modeling the border as two coupled stiffness elements, the present framework distinguishes between 'hardening' the rigid subsystem and 'smoothing' the transition. Cement augmentation of the UIV screw–bone interface increases K_s. While this can improve immediate fixation strength and pull-out resistance, Eq. (1) shows that increasing K_s (with K_a held constant) tends to increase the fraction of applied moment carried by the screw–rod complex, potentially accelerating toggling under cyclic loading. In addition, cement-augmented pedicle screws have well-described risks, including cement leakage and challenging revision scenarios, and may shift failure cranially via adjacent insufficiency fracture in susceptible patients [5].

UIV+1 augmentation targets the complementary variable—K_a—thereby reducing the screw's moment share (Eq. 2) while simultaneously increasing local foundation stiffness k, which localizes deformation (Eq. 3). Conceptually, this is impedance matching: rather than steepening the stiffness cliff at the construct edge, it raises the impedance of the cranial element and smooths the gradient. This choice is consistent with the clinical intuition that the junction fails where motion and stiffness are mismatched, and it provides a mechanism-constrained explanation for why prophylactic vertebroplasty approaches at UIV and/or UIV+1 have shown potential benefit in selected series [1-3], within the broader landscape of junctional prevention strategies [4].

Material choice and execution matter because the goal is controlled structural reprogramming, not maximal filling. High-viscosity PMMA supports slow, controlled injection and has been associated with reduced leakage compared with lower-viscosity approaches in vertebroplasty contexts [6,7].

Low-temperature/low-exotherm considerations are particularly relevant when augmenting an uninstrumented vertebra adjacent to neural elements and endplates, and low-exotherm formulations have been proposed to mitigate thermal risk [8]. In an interface-smoothing strategy, excessive cement volume, endplate violation, or asymmetric filling could create stress risers that undermine the intended benefit; thus, central trabecular reinforcement with careful fluoroscopic monitoring is mechanistically aligned with Eqs. (2)–(3).

The limitations of the present work are important. The models are intentionally simple: they assume linear elastic behavior, small rotations, and a sagittal-plane representation. The true junction is three-dimensional, with contributions from rod contouring, facet loading, ligament tension, and patient-specific global alignment. Moreover, the effective stiffness multiplier α is not directly measured in this report and will depend on baseline bone quality, cement volume and distribution, and vertebral geometry. The current radiographic material is illustrative rather than comparative, and therefore cannot establish effect size or clinical superiority. Prospective, controlled evaluation should quantify not only radiographic endpoints ($\Delta\varphi$, $d_{head–EP}$, halo) but also patient-centered outcomes and complications, with stratification by osteoporosis severity and construct characteristics.

Despite these caveats, a mechanics-first framing can be pragmatically useful. Junctional failure is often experienced clinically as partly unpredictable—similar constructs can fail differently across patients. One way to reduce this sensitivity is to engineer a more forgiving boundary condition. By modestly increasing K_a and k at UIV+1, the junction may become less dependent on small variations in patient biology and daily loading, creating a 'pocket of reducibility' in which the dominant mechanics are simpler and more robust. In that sense, mathematics is not an abstraction but a design tool: it specifies the direction of intervention and yields falsifiable predictions that radiographs and clinical follow-up can confirm or refute.

Conclusions

Proximal junctional complications after posterior lumbar instrumentation can be reframed as a predictable consequence of impedance mismatch at an abrupt stiffness transition. A first-principles moment-sharing model predicts that increasing the stiffness of the proximal adjacent vertebra (UIV+1) reduces the moment carried by the UIV screw-rod complex by a quantifiable factor (Eq. 2), and a beam-on-elastic-foundation model predicts more localized cranial load transfer after augmentation (Eq. 3). Crucially, the governing equations reveal a nonlinearity in therapeutic benefit—a law of diminishing returns. This mathematical property implies that moderate stiffening captures

the majority of the offloading effect without requiring rigid equivalence, thereby validating a "minimum effective dose" strategy that prioritizes safety over maximal filling. UIV+1 cement augmentation, performed with controlled, high-viscosity and low-temperature PMMA, is therefore positioned as a minimally invasive, physics-guided strategy to smooth the stiffness gradient at the construct edge, potentially reducing screw toggling, endplate encroachment, and adjacent failure without routine proximal extension.

References

1. Raman T, Miller E, Martin CT, et al. The effect of prophylactic vertebroplasty on the incidence of proximal junctional kyphosis and proximal junctional failure following posterior spinal fusion in adult spinal deformity: a 5-year follow-up study. Spine J. 2017; 17: 1489-1498.
2. Ghobrial GM, Eichberg DG, Kolcun JPG, et al. Prophylactic vertebral cement augmentation at the uppermost instrumented vertebra and rostral adjacent vertebra for prevention of proximal junctional kyphosis/failure after long-segment fusion for adult spinal deformity. Spine J. 2017; 17: 1499-1505.
3. Doodkorte RJP, Vercoulen TFG, Roth AK, et al. Instrumentation techniques to prevent proximal junctional kyphosis and proximal junctional failure in adult spinal deformity correction: a systematic review of biomechanical studies. Spine J. 2021; 21: 842-854.
4. Vercoulen TFG, Doodkorte RJP, Roth AK, et al. Instrumentation techniques to prevent proximal junctional kyphosis and proximal junctional failure in adult spinal deformity correction: a systematic review of clinical studies. Global Spine J. 2022; 12: 1282-1296.
5. Boucas P, Mamdouhi T, Rizzo SE, et al. Cement augmentation of pedicle screw instrumentation: a literature review. Asian Spine J. 2023; 17: 939-948.
6. Georgy BA. Clinical experience with high-viscosity cements for percutaneous vertebral body augmentation: occurrence, degree, and location of cement leakage compared with kyphoplasty. AJNR Am J Neuroradiol. 2010; 31: 504-508.
7. Wang J, Zhang J, Huang J, et al. Clinical effect analysis of vertebroplasty with high viscosity and standard bone cement for Kummell disease. Medicine Baltimore. 2024; 103: e39960.
8. Szoradi GT, Feier AM, Zuh SG, et al. Polymethyl methacrylate bone cement polymerization induced thermal necrosis at the cement–bone interface: a narrative review. Applied Sciences. 2024; 14: 11651.